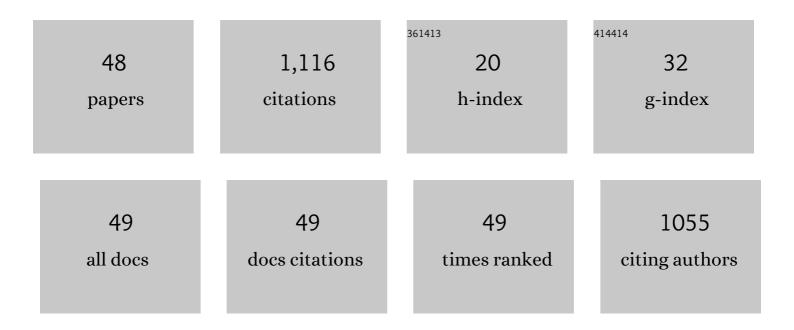
VladimÃ-r Sychrovský

List of Publications by Year in descending order

Source: https://exaly.com/author-pdf/6944391/publications.pdf Version: 2024-02-01



#	Article	IF	CITATIONS
1	Structures, physicochemical properties, and applications of T–Hg ^{II} –T, C–Ag ^I –C, and other metallo-base-pairs. Chemical Communications, 2015, 51, 17343-17360.	4.1	136
2	The structure of metallo-DNA with consecutive thymine–HgII–thymine base pairs explains positive entropy for the metallo base pair formation. Nucleic Acids Research, 2014, 42, 4094-4099.	14.5	106
3	Structure Determination of an Ag ^I â€Mediated Cytosine–Cytosine Base Pair within DNA Duplex in Solution with ¹ H/ ¹⁵ N/ ¹⁰⁹ Ag NMR Spectroscopy. Chemistry - A European Journal, 2016, 22, 13028-13031.	3.3	63
4	Chemical Shifts in Nucleic Acids Studied by Density Functional Theory Calculations and Comparison with Experiment. Chemistry - A European Journal, 2012, 18, 12372-12387.	3.3	54
5	Formation of a Thymineâ€Hg ^{II} â€Thymine Metalâ€Mediated DNA Base Pair: Proposal and Theoretical Calculation of the Reaction Pathway. Chemistry - A European Journal, 2013, 19, 9884-9894.	3.3	45
6	Raman spectroscopic detection of the T-Hg II -T base pair and the ionic characteristics of mercury. Nucleic Acids Research, 2012, 40, 5766-5774.	14.5	44
7	Theoretical Calculation of the NMR Spinâ^'Spin Coupling Constants and the NMR Shifts Allow Distinguishability between the Specific Direct and the Water-Mediated Binding of a Divalent Metal Cation to Guanine. Journal of the American Chemical Society, 2004, 126, 663-672.	13.7	41
8	Theoretical and Experimental Study of Charge Transfer through DNA: Impact of Mercury Mediated T-Hg-T Base Pair. Journal of Physical Chemistry B, 2014, 118, 5374-5381.	2.6	41
9	Limits in Proton Nuclear Singletâ€State Lifetimes Measured with <i>para</i> â€Hydrogenâ€Induced Polarization. ChemPhysChem, 2016, 17, 2967-2971.	2.1	38
10	Interactions of hydrated divalent metal cations with nucleic acid bases. How to relate the gas phase data to solution situation and binding selectivity in nucleic acids. Physical Chemistry Chemical Physics, 2004, 6, 2772-2780.	2.8	36
11	Direct detection of the mercury–nitrogen bond in the thymine–Hg ^{II} –thymine base-pair with ¹⁹⁹ Hg NMR spectroscopy. Chemical Communications, 2015, 51, 8488-8491.	4.1	36
12	Structure and Dynamics of the ApA, ApC, CpA, and CpC RNA Dinucleoside Monophosphates Resolved with NMR Scalar Spina [^] Spin Couplings. Journal of Physical Chemistry B, 2009, 113, 1182-1191.	2.6	33
13	On the role of mercury in the non-covalent stabilisation of consecutive U–Hg ^{II} –U metal-mediated nucleic acid base pairs: metallophilic attraction enters the world of nucleic acids. Physical Chemistry Chemical Physics, 2011, 13, 100-103.	2.8	33
14	Revisiting the planarity of nucleic acid bases: Pyramidilization at glycosidic nitrogen in purine bases is modulated by orientation of glycosidic torsion. Nucleic Acids Research, 2009, 37, 7321-7331.	14.5	27
15	Sugar Pucker Modulates the Cross-Correlated Relaxation Rates across the Glycosidic Bond in DNA. Journal of the American Chemical Society, 2005, 127, 14663-14667.	13.7	24
16	Calculation of Structural Behavior of Indirect NMR Spinâ^'Spin Couplings in the Backbone of Nucleic Acids. Journal of Physical Chemistry B, 2006, 110, 22894-22902.	2.6	24
17	Raman spectroscopy and DFT calculations of PEDOT:PSS in a dipolar field. Physical Chemistry Chemical Physics, 2021, 24, 541-550.	2.8	24
18	Exploring the Structure of a DNA Hairpin with the Help of NMR Spinâ^'Spin Coupling Constants:Â An Experimental and Quantum Chemical Investigation. Journal of Physical Chemistry B, 2002, 106, 10242-10250.	2.6	22

#	Article	IF	CITATIONS
19	Correlating the ³¹ P NMR Chemical Shielding Tensor and the ² <i>J</i> ,Sub>P,C Spin–Spin Coupling Constants with Torsion Angles ζ and α in the Backbone of Nucleic Acids. Journal of Physical Chemistry B, 2012, 116, 3823-3833.	2.6	22
20	Indirect NMR Spinâ^'Spin Coupling Constants 3J(P,C) and 2J(P,H) across the Pâ^'O··Ĥâ^'C Link Can Be Used for Structure Determination of Nucleic Acids. Journal of the American Chemical Society, 2006, 128, 6823-6828.	13.7	21
21	Calculating the Response of NMR Shielding Tensor σ(³¹ P) and ² <i>J</i> (³¹ P, ¹³ C) Coupling Constants in Nucleic Acid Phosphate to Coordination of the Mg ²⁺ Cation. Journal of Physical Chemistry A, 2011, 115, 2385-2395.	2.5	21
22	Detection of Mercury–TpT Dinucleotide Binding by Raman Spectra: A Computational Study. Journal of Physical Chemistry A, 2012, 116, 8313-8320.	2.5	19
23	HgII/AgI-mediated base pairs and their NMR spectroscopic studies. Inorganica Chimica Acta, 2016, 452, 34-42.	2.4	19
24	The mechanism of the glycosylase reaction with hOGG1 base-excision repair enzyme: concerted effect of Lys249 and Asp268 during excision of 8-oxoguanine. Nucleic Acids Research, 2017, 45, 5231-5242.	14.5	19
25	The effect of water on NMR spin–spin couplings in DNA: Improvement of calculated values by application of two solvent models. Physical Chemistry Chemical Physics, 2003, 5, 734.	2.8	18
26	The benchmark of ³¹ P NMR parameters in phosphate: a case study on structurally constrained and flexible phosphate. Physical Chemistry Chemical Physics, 2017, 19, 31830-31841.	2.8	17
27	Structural Interpretation of J Coupling Constants in Guanosine and Deoxyguanosine: Modeling the Effects of Sugar Pucker, Backbone Conformation, and Base Pairing. Journal of Physical Chemistry A, 2009, 113, 8379-8386.	2.5	15
28	Pyramidalization of the Glycosidic Nitrogen Provides the Way for Efficient Cleavage of the N-Glycosidic Bond of 8-OxoG with the hOGG1 DNA Repair Protein. Journal of Physical Chemistry B, 2012, 116, 12535-12544.	2.6	13
29	Theoretical Study of the Scalar Coupling Constants across the Noncovalent Contacts in RNA Base Pairs:  The cis- and trans-WatsonⰠCrick/Sugar Edge Base Pair Family. Journal of Physical Chemistry B, 2007, 111, 10813-10824.	2.6	12
30	Charge transfer through DNA/DNA duplexes and DNA/RNA hybrids: Complex theoretical and experimental studies. Biophysical Chemistry, 2013, 180-181, 127-134.	2.8	11
31	Structural interpretation of the ³¹ P NMR chemical shifts in thiophosphate and phosphate: key effects due to spin–orbit and explicit solvent. Physical Chemistry Chemical Physics, 2019, 21, 9924-9934.	2.8	11
32	Benchmark Theoretical and Experimental Study on ¹⁵ N NMR Shifts of Oxidatively Damaged Guanine. Journal of Physical Chemistry B, 2016, 120, 915-925.	2.6	10
33	B <i>_k</i> approximation applied to CI-SDTQ. Molecular Physics, 1996, 88, 1137-1142.	1.7	8
34	Evaluating the Effects of the Nonplanarity of Nucleic Acid Bases on NMR, IR, and Vibrational Circular Dichroism Spectra: A Density Functional Theory Computational Study. Journal of Physical Chemistry A, 2010, 114, 10202-10208.	2.5	8
35	Guanine Bases in DNA G-Quadruplex Adopt Nonplanar Geometries Owing to Solvation and Base Pairing. Journal of Physical Chemistry A, 2012, 116, 4144-4151.	2.5	7
36	Probing the Flexibility of Internal Rotation in Silylated Phenols with the NMR Scalar Spinâ^'Spin Coupling Constants. Journal of Physical Chemistry A, 2008, 112, 5167-5174.	2.5	6

#	Article	IF	CITATIONS
37	The activation of N-glycosidic bond cleavage performed by base-excision repair enzyme hOGG1; theoretical study of the role of Lys 249 residue in activation of G, OxoG and FapyG. RSC Advances, 2014, 4, 44043-44051.	3.6	6
38	Impact of nucleic acid self-alignment in a strong magnetic field on the interpretation of indirect spin–spin interactions. Journal of Biomolecular NMR, 2016, 64, 53-62.	2.8	6
39	Bk approximation applied to the multireference configuration interaction method. International Journal of Quantum Chemistry, 2000, 76, 185-196.	2.0	5
40	The <scp>Adâ€MD</scp> method to calculate <scp>NMR</scp> shift including effects due to conformational dynamics: The <scp>³¹P NMR</scp> shift in <scp>DNA</scp> . Journal of Computational Chemistry, 2022, 43, 132-143.	3.3	5
41	Ascorbigen A—NMR identification. Magnetic Resonance in Chemistry, 2019, 57, 1084-1096.	1.9	3
42	The effect of chemical modification of DNA base on binding of HgII and AgI in metal-mediated base pairs. Inorganica Chimica Acta, 2016, 452, 199-204.	2.4	2
43	Interstrand Charge Transport within Metallo-DNA: the Effect Due to Hg(II)- and Ag(I)-Mediated Base Pairs. Journal of Physical Chemistry C, 2020, 124, 7477-7486.	3.1	2
44	FTIR Measurement of the Hydrogenated Si(100) Surface: The Structure-Vibrational Interpretation by Means of Periodic DFT Calculation. Journal of Physical Chemistry C, 2021, 125, 9219-9228.	3.1	2
45	QM and QM/MM umbrella sampling MD study of the formation of Hg(II)–thymine bond: Model for evaluation of the reaction energy profiles in solutions with constant pH. Journal of Computational Chemistry, 2020, 41, 1509-1520.	3.3	1
46	2P119 Nitrogen-15 NMR spectroscopic studies of Ag(I)-mediated C-C base-pairs(05A. Nucleic acid:) Tj ETQq0 0 0 Seibutsu Butsuri, 2014, 54, S214.	rgBT /Ove 0.1	rlock 10 Tf 5 0
47	HERMES – A Software Tool for the Prediction and Analysis of Magneticâ€Fieldâ€Induced Residual Dipolar Couplings in Nucleic Acids. ChemPlusChem, 2020, 85, 2177-2185.	2.8	0

48Quantitative Analysis of Nanorough Hydrogenated Si(111) Surfaces through Vibrational Spectral
Assignment by Periodic DFT Calculations. Journal of Physical Chemistry C, 2022, 126, 8278-8286.3.10